Finite Element Study of the Effect of Substrate Properties in Micro-cutting Thin Workpiece Materials

2016 IOP Conf. Ser.: Mater. Sci. Eng. 114 012005

(http://iopscience.iop.org/1757-899X/114/1/012005)

Finite Element Study of the Effect of Substrate Properties in Micro-cutting Thin Workpiece Materials

K Saptaji[1] and S Subbiah[2]

[1]Faculty of Manufacturing Engineering, University Malaysia Pahang, 26600 Pekan, Malaysia
[2]Department of Mechanical Engineering, Indian Institute of Technology Madras, 600036 Chennai, India

E-mail: kushendarsyah@ump.edu.my

Abstract. The cutting mechanism and residual stress profile of the micro-cutting thin workpiece are affected by the interaction of the thin workpiece and the fixture (substrate) underneath it similar to that observed in the nano-indentation and nano-scratching of thin film. The appropriate substrate properties are necessary especially to avoid detachment during machining and to minimize deformation and warping of the machined thin workpiece. Thus, the investigations of the influence of substrate properties on micro-cutting thin workpiece are essentially to be conducted. The finite element study of orthogonal micro-cutting of thin Al6061-T6 is presented here. The simulations were conducted to study the residual stress profile across the thickness of the machined thin workpiece at various workpiece thicknesses and various substrate (adhesive) elastic properties. Simulations results show that as the machined workpiece become thinner, the stress is more significant not only on the machined surface but also it can reach the bottom of the workpiece. The stiffer substrate produces less variation of the stress across the workpiece thickness while more compliant substrate produces broader stress variation as the workpiece become thinner. The results show the significant effect of the workpiece thickness and the substrate properties on the stress profiles in the micro-cutting of thin workpiece.

1. Introduction

Investigations in micro-cutting thin workpieces (i.e. where the depth of cut may be comparable to workpiece thickness) are rare while those in micro-cutting thick workpieces are widely reported. In the machining of thick workpiece, the ratio of depth of cut (t_0) to the machined workpiece thickness (t_w) is very small, and the depth of deformation beneath the tool in to the workpiece thickness is also usually insignificant. The deformation induced by machining process may be more significant in the thinner workpiece. In the thin workpiece, the ratio of t_0 to t_w is larger; hence the plastic deformation in the form of stress produced by the tool may transmit through the thin workpiece, i.e. reach the bottom of the workpiece and interacts with the interface of the workpiece and fixture (Figure 1). If the stress is high enough it can pass through the fixture (substrate) or deflect back and furthermore produce enhanced stresses or deformation; if the stresses are larger than the strength of the fixture it can lead to detachment (slip-off) of the workpiece.

[1] To whom any correspondence should be addressed.

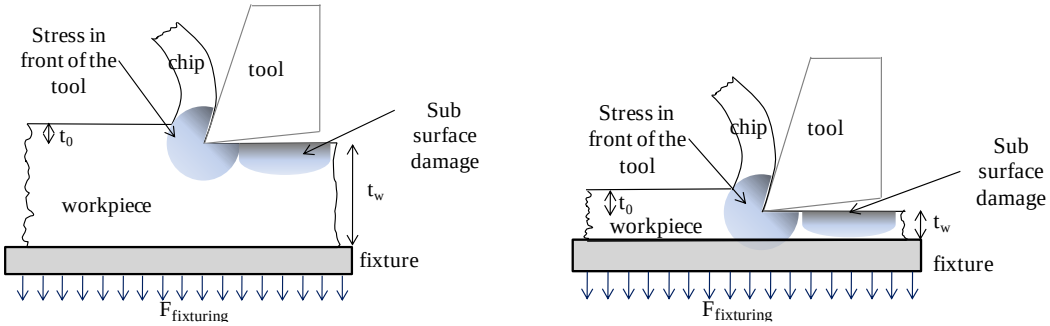

Figure 1. Illustration of the cutting process on thick workpiece (left) and thin workpiece (right). In a thin workpeice t_w is comparable to t_o.

The cutting mechanism and plastic deformation of the thin workpiece is also affected by the interaction of the thin workpiece and the substrate underneath it similar to that observed in the nano-indentation and nano-scratching of thin film [1]. The appropriate fixturing method and properties are necessary to minimize the deformation induced, to avoid detachment during machining [2] and to minimize warping after thin workpiece released from the fixture. Thus, the investigations of the influence of substrate properties in the cutting mechanism and residual stress profile especially for thin workpiece conditions are essentially to be conducted. The residual stress profile can be used as one of the parameters to study the effects of the workpiece fixture on the machining process and to indicate the severity of warping. However, the measurement of the residual stress profile in a free thin work material with the thickness of about 50 μm is still a challenge because the thin workpiece is very delicate. Hence, finite element analysis is necessary to be conducted. The finite element model developed in ABAQUS 6.9-2 is utilized to study the effect of workpiece thickness and the contribution of the substrate properties on the residual stress profile of the machined workpiece especially in thin conditions. Different elastic properties of the substrate can give different stress variations across the workpiece which in the end can affect the shape of the workpiece when the workpiece is released from the fixture.

2. Finite element model

The three dimensional (3D) orthogonal cutting model is developed using eight-node brick trilinear coupled thermal-stress (C3D8RT) element and a Lagrangian method. Figure 2 shows the model setup and boundary conditions for 20 μm workpiece thickness. Smaller element sizes are used for 10 μm thick; starting from the top of the workpiece with a size of 0.625 μm x 1.25 μm, whereas the element size of the adhesive is 1 μm x 2 μm. In order to reduce the simulation time, the width of the workpiece is considered to be 0.5 μm consisting of one element thick. The process is assumed to be plane strain because the width of the orthogonal process workpiece is more than 5 times of the thickness. The workpiece is held fixed while cutting tool moves horizontally towards the workpiece with a fixed depth of cut (t_0) 5 μm. The left and right sides are constrained in the direction perpendicular to the cutting speed, while the back side of the workpiece is fixed in all directions. Four final workpieces thickness (t_w) values of 5, 10 μm, 50 μm, and 80 μm are used in order to observe differences between thin and thick workpiece machining conditions. The substrate is modelled below the workpiece with the fixed thickness of 30 μm. The interface between the metal and substrate is modelled using tie-constraint so that the two materials are assumed to be perfectly bonded. This assumption is made because we have seen the detachment of the thin workpiece at the ratio of t_0/t_w about 0.1 in the incipient chip formation where sudden increase in the load occurs [2]. However in this case the process is assumed to be in steady state condition, where the detachment is assumed not to occur. In this simulation, higher cutting speed is applied similar to the experimental data (from literature) used in the validation of the material separation criterion for Al-6061-T6 [3]. A complete set of cutting parameters used is shown in the Table 1.

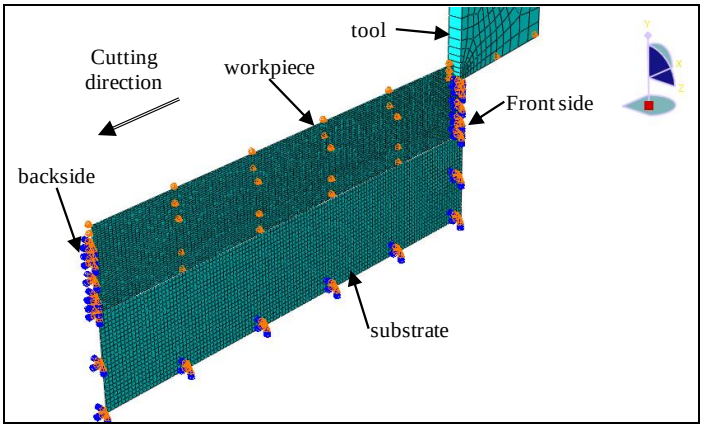

Figure 2. Element mesh and boundary conditions for 20 μm workpiece thickness.

Table 1. Simulation Parameters

Workpiece	Al6061-T6
Tool	Single Crystal Diamond
Tool rake angle and clearance angle	1^0 and 4.5^0
Cutting speed (m/sec)	30
Depth of cut (t_0) (μm)	5
Substrate thickness (μm)	30
Substrate Elastic Modulus (E_s) (GPa)	275.6; 6.89; 2.206; 0.689
E_W/E_S (Elastic Modulus ratio)	0.25, 10, 31, 100
Machined workpiece thickness (t_w) (μm)	5, 10, 50, 80
t_0/t_w	0.0625, 0.1, 0.5, 1

2.1. Materials properties

The workpiece, tool and substrate properties used are shown in Table 2, Table 3 and Table 4 respectively. The workpiece used is Aluminium Al6061-T6, the tool used is Single Crystal Diamond (SCD), and the substrate is adhesive Dymax® 6-621. The application of adhesive as the fixturing method in the manufacturing process especially machining process has been reported in literature for thick and complex shape workpiece [4] as well as for thin workpiece [5]. The use of adhesive types can give thin, uniform bonding layer and can be removed easily after machining is completed. Here, the elastic modulus of the metal is fixed (the elastic modulus of Al6061-T6), while the elastic modulus of the substrate is varied in order to get different combination of the ratio of elastic modulus of workpiece (E_W) and elastic modulus of substrate (E_S) as shown in Table 1. Therefore the other substrate properties remain the same as in Table 4. The E_W/E_S ratios are defined to cover the stiff substrate (high substrate elastic modulus) for the case of E_W/E_S = 0.25 and flexible substrate (low substrate elastic modulus) for the case of E_W/E_S = 10, 31 and 100 respectively. The Johnson-Cook (J-C) constitutive model is used as the workpiece material model.

Table 2. Workpiece material properties (Al6061-T6) [6][7][8]

Density (kg/m^3)	2,700
Specific heat (J/kg K)	896.0
Thermal conductivity (W/m K)	167.0
Coefficient of thermal expansion ($^oC^{-1}$)	25.2×10^{-6}
Young's modulus (E_w) (GPa)	68.9
Poisson's ratio	0.33
Melting temperature (^oC)	582
Johnson-Cook strength model	A=324.0 MPa, B=114.0 MPa, n=0.42, C=0.002, m=1.34
Johnson-Cook failure parameters [7]	d_1=0.071, d_2=1.248, d_3=-1.142, d_4=0.147, d_5=0.0

Table 3. Tool material properties (SCD) [8]

Density (kg/m^3)	3,500
Specific heat (J/kg K)	0.4715
Thermal conductivity (W/m K)	2,000
Coefficient of thermal expansion ($^oC^{-1}$)	1.18 x 10^{-6}
Young's modulus (GPa)	850
Poisson's ratio	0.1

Table 4. Adhesive material properties (Dymax® 6-621).

Density (kg/m^3)	1,066
Specific heat (J/kg K)	0.263
Coefficient of thermal expansion ($^oC^{-1}$)	9 x 10^{-6}
Young's modulus (GPa)	2.206
Poisson's ratio	0.25 – 0.35
Tensile Lap Shear strength (steel-steel) (MPa)	24.82
Tensile at Break (MPa)	35.9
Elongation at Break (%)	35

2.2. Material separation criterion and failure model

Johnson-Cook (J-C) shear failure model is used to model chip formation [9] and to overcome the used of separation criteria and predefined fracture line. The Johnson-Cook failure parameters (d_1 to d_5) for Al6061-T6 are taken from literature [7] and given in Table 2. The experimentally measured cutting force and thrust force values from the literature [3] of high speed cutting for Al6061-T61 are used for the validation of the J-C failure parameters values. The cutting conditions are shown in Table 5.

Table 5. Cutting conditions for model validation [3]

Tool materials	Rake angle	Width of cut	Depth of cut	Cutting speed
D2 tool steel	5.5^o	10.1 mm	0.25 mm	30 m/s

The results of the validation using the J-C failure parameters from [7] reveal that the forces simulated match with the experimental results within an error, in cutting force of about 14.03% and thrust force of about 8.9%. However, failure is seen to occur at damage parameter (ω) value of 0.6 (and not 1.0). Based on this comparison the model is well validated and the failure parameters are reasonable to be used in the simulations.

2.3. Chip-tool interaction

The friction conditions proposed by Zorev [10] is used in this model. The parameters for the friction conditions are determined to be τ_p=300 MPa and μ=0.25 [11].

2.4. Heat transfer

The thermal properties values of the Al6061-T6 and SCD tool are listed in the Table 2 and Table 3. It is assumed that 90% of energy dissipated by plastic deformation is converted into heat [12] and heat is mainly generated in an element by plastic work [13].

3. Simulation results and discussion

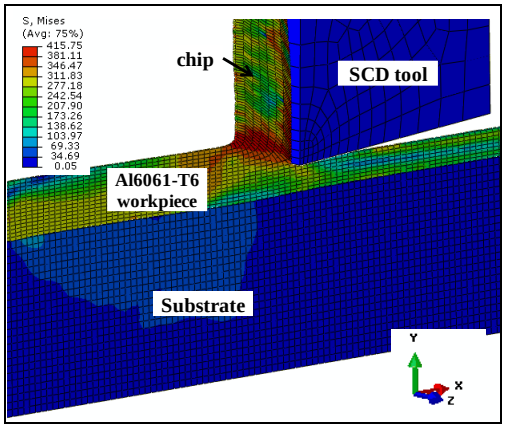

Figure 3. ABAQUS simulation for the chip formation process.

Figure 3 shows a steady state situation in one of the 3D orthogonal cutting condition simulated. Once steady state in the cutting process is achieved, the maximum deformation is seen to occur in the shear zone extending from the edge of the cutting tool to the junction between the undeformed workpiece and the deformed chip, known as the primary deformation region. As the tool move towards the workpiece during the cutting process, stresses in front of the tool and perpendicular with the cutting direction are also generated. As the tool leaves the machined area, it leaves behind a deformed zone at the surface and subsurface.

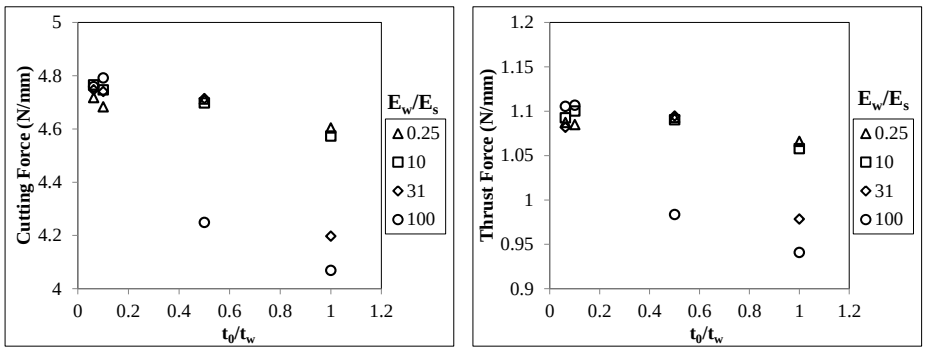

Figure 4. Cutting force (left) and thrust force (right) for various ratio of E_W/E_S.

Force values are extracted from the simulation when the steady state cutting process is achieved (Figure 4). In general, the cutting force ranges between 4.07 to 4.79 N/mm and the thrust force between 0.94 to 1.11 N/mm. Both the cutting force and the thrust force values are widely diverged as the t_0/t_w increased especially for the t_0/t_w = 0.5 and 1. These force variations may occur due to the significant effect of the elastic modulus of the substrate especially when the workpiece becomes thinner. The cutting force and thrust force values are the lowest for the case of E_W/E_S = 100 when the t_0/t_w are 0.5 and 1. The lower substrate elastic modulus (E_W/E_S = 100) causing higher displacement due to the more compliant properties of the substrate which affect the cutting process producing low value of forces.

3.1. Loading from the tool during steady state machining

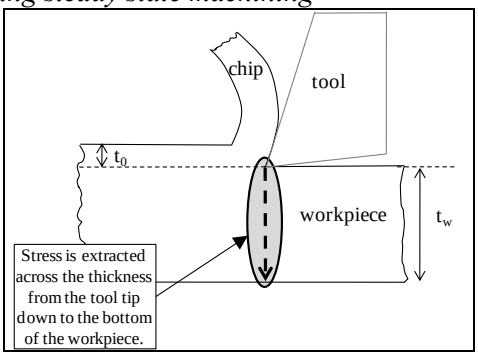

Figure 5. Illustration of the location where the stress is extracted from the workpiece. The stress is extracted across the thickness of the workpiece from below the tool tip down to the bottom of the workpiece.

The stress values parallel to the cutting feed direction (S11) across the workpiece thickness of the machined thin workpiece may corroborates the warping to be occurred after the thin workpiece released from the fixture [14]. Hence this stress is extracted from the simulation across the thickness of the workpiece at each nodal point down to the bottom of the workpiece during steady state cutting condition and after the tool leaves the workpiece with the boundary conditions remained intact (Figure 5). The stress distributions across the workpiece thickness at steady state condition for different ratio of depth of cut (t_0) to the machined workpiece thickness (t_w) are shown in Figure 6. The y axis representing the loading stress from the cutting tool on the workpiece is plotted using the same axis scale for the four graphs for ease of observations. The x-axis represents the distance from the machined surface (tool tip) until the bottom of the workpiece (interface with the substrate).

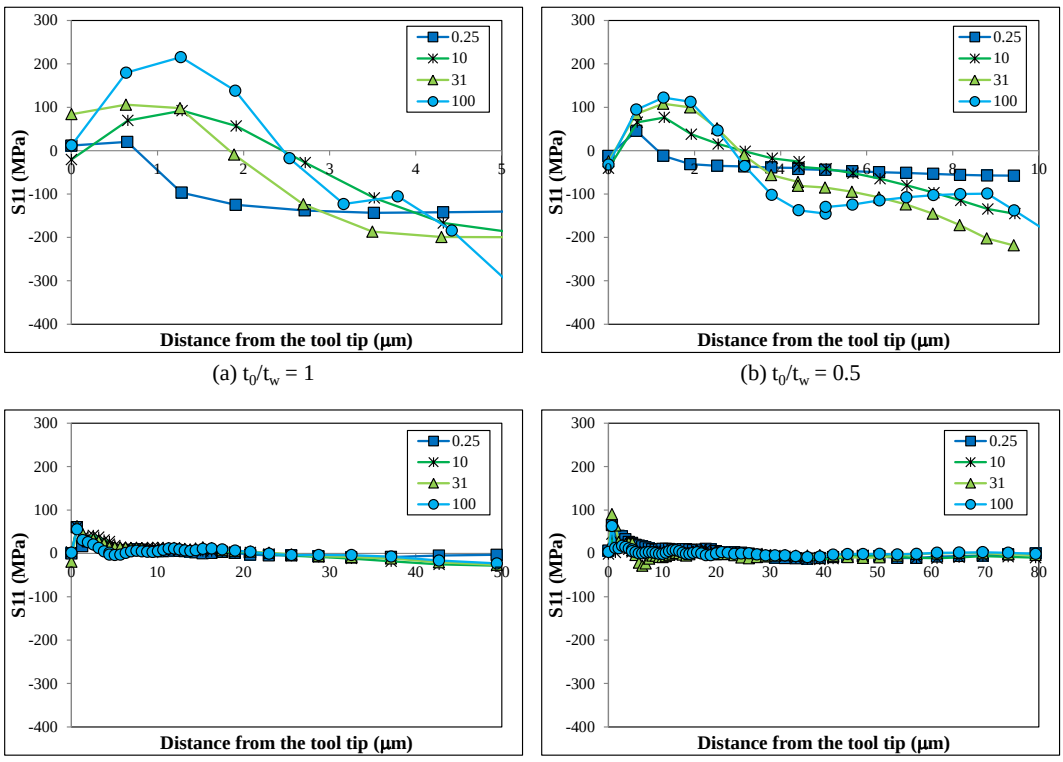

(a) $t_0/t_w = 1$ (b) $t_0/t_w = 0.5$

(c) $t_0/t_w = 0.1$ (d) $t_0/t_w = 0.0625$

Figure 6. Stress profile parallel with the cutting direction across the workpiece thickness below the tool tip at steady state condition plotted for different E_W/E_S ratio at various t_0/t_w.

In general, the stress profiles are tensile near the tool tip for all the elastic modulus ratios and have the maximum value at the depth about 1 – 5 μm from the tool tip for all values of t_0/t_w. The stress profile across the thickness of the workpiece is likely to have an S-shape curve that varies from tensile near the tool tip and turn gradually to be compressive into the bottom workpiece with the turning point near the middle section when $t_0/t_w = 1$ especially for $E_W/E_S > 1$ (compliant substrate) (Figure 6 (a)). The $E_W/E_S = 100$ has the highest tensile stress at the depth of about 1.5 μm and has the most compressive stress at the bottom of the workpiece. The $E_W/E_S = 0.25$ has lower stress value and less stress profile variation across the thickness compared to other E_W/E_S especially when $t_0/t_w = 0.5$ and $t_0/t_w = 1$ (Figure 6 (a) and (b)). The significant different of the stress profile for $E_W/E_S = 0.25$ especially in $t_0/t_w = 0.5$ and $t_0/t_w = 1$ can occur due to the effect of the stiff substrate, in which the stress is not penetrated deeper into the substrate and eventually is dissipated. The $E_W/E_S = 31$ and 100 have the highest tensile stress near the tool tip but the $E_W/E_S = 31$ is the most compressive compared to other E_W/E_S especially at the bottom of workpiece (more compressive) when $t_0/t_w = 0.5$ (Figure 6 (b)). In the case of $t_0/t_w = 0.1$ and 0.0625, the stress values are relatively the same just below the tool tip and increased to be more tensile in the vicinity of the tool tip and turn gradually to be smaller toward the bottom of the workpiece (Figure 6 (c) and (d)). For $t_0/t_w = 0.1$ and 0.0625, the high tensile stress occurs down to the depth about 3 – 5 μm resulting in the ratio of the depth of deformation to the workpiece thickness are about 0.1, and 0.0625 for t_0/t_w of 0.1, and 0.0625 respectively.

3.2. Substrate effects during steady state cutting conditions

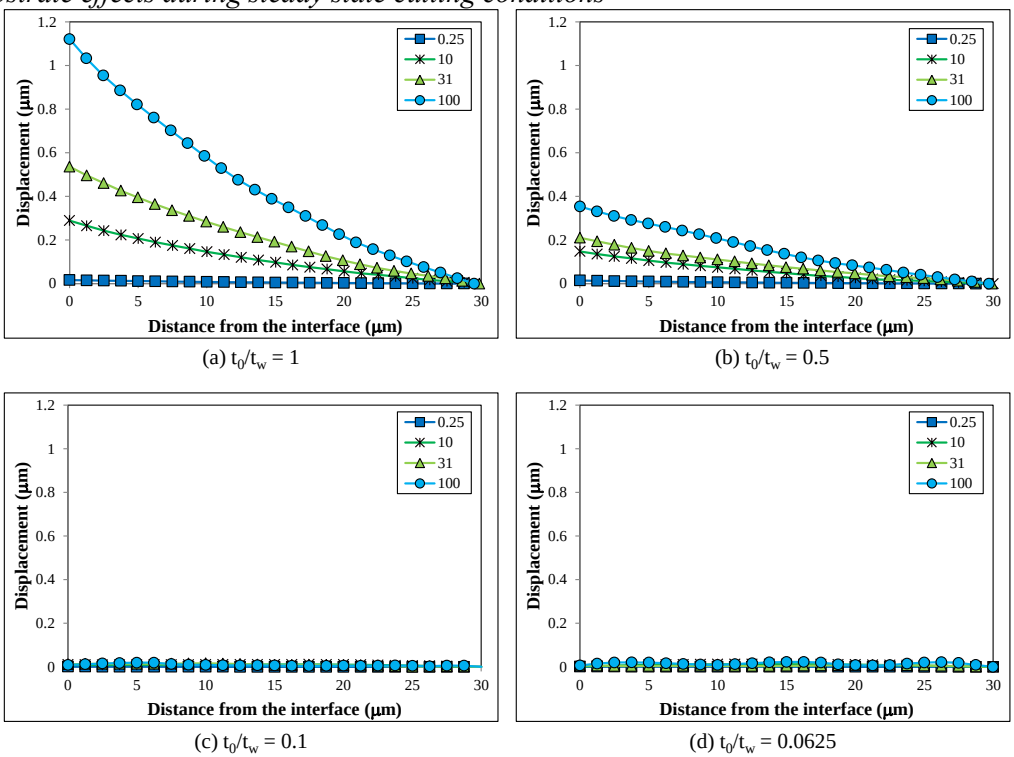

(a) $t_0/t_w = 1$ (b) $t_0/t_w = 0.5$

(c) $t_0/t_w = 0.1$ (d) $t_0/t_w = 0.0625$

Figure 7. Displacement profile across the substrate at steady state cutting condition plotted for different E_W/E_S ratio at various t_0/t_w.

The observation of the substrate displacement during steady state cutting conditions just below the tool tip is important in order to understand the contribution of substrate elastic properties to the cutting mechanisms (Figure 7). Similar with Figure 6 the four graphs shown in Figure 7 are applied using the same y-axis scale for the displacement while the x-axis represented the distance from the interface.

In general, the displacement increases as the t_0/t_w and E_W/E_S increased. For the case of $t_0/t_w = 1$ and 0.5, the displacement increases as the E_W/E_S increased, and it is the largest at the interface and as

going deeper it reduces to zero (Figure 7 (a) and (b)). In contrast, when t_0/t_w = 0.1 and 0.0625 the displacements are very small compared to t_0/t_w = 1 and 0.5 (Figure 7 (c) and (d)). In addition, it can be observed that for E_W/E_S = 0.25 displacement is very low compared to others especially when t_0/t_w = 1 and 0.5 due to the effect of the stiff substrate. The compliant substrate is seen to produce more displacement and furthermore influences the forces especially for thinner workpiece conditions (t_0/t_w = 1 and 0.5). This can be observed especially for the case of E_W/E_S = 100 where the forces are lower than for other elastic modulus ratios (Figure 4). While E_W/E_S = 0.25 (stiffer substrate) has much less displacement which shows no significant changes of the forces at different t_0/t_w ratios. The observations are similar to those observe in the nano-indentation of thin film where the film will sink-in if the substrate is compliant, whereas stiffer substrates enhance the plastic flow of the film [1]. The substrate properties are seen to have less significant effect on the cutting mechanism in the case of thicker workpiece conditions (t_0/t_w = 0.1 and 0.0625) shown by the low displacement (Figure 7), low stress values near the interface of the workpiece and substrate (Figure 6) and less varied forces values (Figure 4). In contrast, the high displacement, more variation of stress across the thickness and more variation of the forces indicate the substrate properties are affected significantly to the cutting mechanism in thinner workpiece conditions (t_0/t_w = 1 and 0.5).

3.3. Residual stress profile after the tool leaves the workpiece

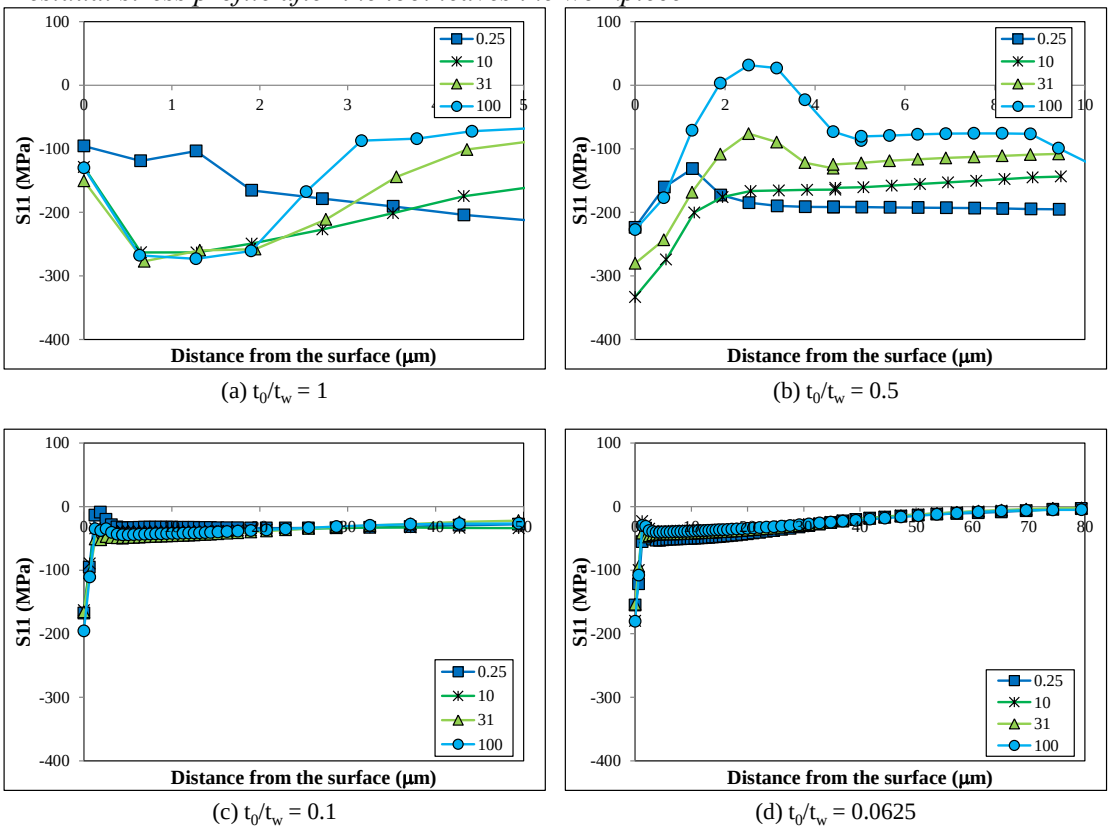

(a) t_0/t_w = 1 (b) t_0/t_w = 0.5

(c) t_0/t_w = 0.1 (d) t_0/t_w = 0.0625

Figure 8. Stress profile parallel with the cutting direction across the workpiece thickness after the tool leaves the workpiece plotted for different E_W/E_S ratio at various t_0/t_w.

The analysis of the stress profiles after the tool leaves the workpiece is also conducted. Figure 8 shows the stress profiles across the workpiece thickness for various E_W/E_S at different t_0/t_w after the tool leaves the workpiece. In general, the compressive stress presents in the machined surface implies that the mechanical or plastic deformation is more dominant in the process [15]. The residual stress profiles across the thickness of the workpiece shown in this condition represent the equilibrium

conditions of the workpiece due to the effect of the substrates where the change of the shapes is accommodated by the substrate.

For the compliant substrate ($E_W/E_S > 1$) when $t_0/t_w = 1$, the stress profile is appeared to be an S-shape curve with the turning point around the middle section and the stress values are still in the compressive state across the thickness with the $E_W/E_S = 100$ having the largest stress range from the top to bottom surfaces (Figure 8 (a)). In contrast, the $E_W/E_S = 0.25$ has lowest compressive stress at the machined surface, turned to become more compressive toward the bottom of the workpiece. The stress values in the machined surface for all the E_W/E_S combination when $t_0/t_w = 0.5$ are higher compared to other combination of t_0/t_w. The stress gradually becomes tensile to the depth of about 2 μm and turn to be compressive again toward to the bottom of the workpiece for $E_W/E_S = 100$ when $t_0/t_w = 0.5$. For $E_W/E_S = 0.25$ the stress become more compressive as deeper into the subsurface and has less stress variation values.

The existence of the high compressive stress only occurs down to the depth of about 3 μm for $t_0/t_w = 0.1$ and 0.0625 for all E_W/E_S, and gradually decreases to become constant which is not significant compared to the thickness (Figure 8 (c) and (d)). Though the stress remains constant, the values do not reach zero for the case of $t_0/t_w = 0.1$ because there may be minor effect from the substrate. This profile is similar with the typical stress profile observed in the result of machining thick workpiece when plastic deformation is more dominant than thermal strain [16] and also the ratio of the depth of deformation to the thickness is not significant. However, the workpiece still possible to experience shape changes in the form of warping after it is released from the substrate especially for the compliant substrate. This is due to the pre-stretch conditions of the machined workpiece when it is held by the compliant substrate.

3.4. Substrate effects after the tool leaves the workpiece

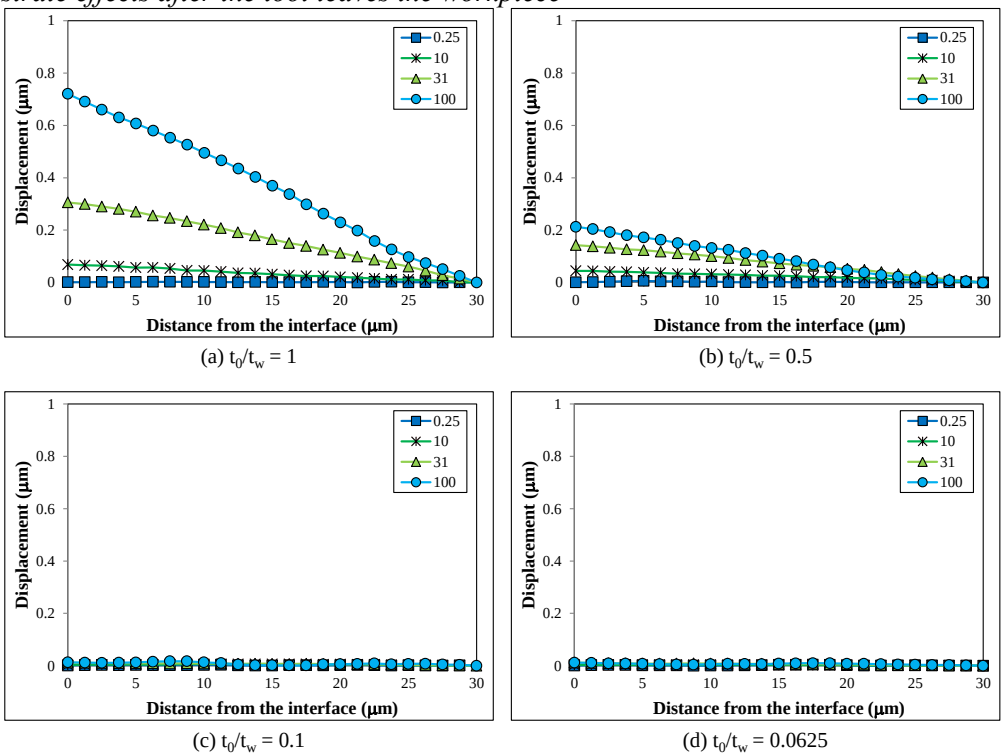

(a) $t_0/t_w = 1$ (b) $t_0/t_w = 0.5$

(c) $t_0/t_w = 0.1$ (d) $t_0/t_w = 0.0625$

Figure 9. Displacement profile across the substrate thickness after the tool leaves the workpiece plotted for different E_W/E_S ratio at various t_0/t_w.

In general, the displacements trends and values of the substrate after the tool leaves the workpiece are similar with those in steady state cutting conditions for all variation of t_0/t_w. Figure 9 shows the displacement profile across the substrate thickness after the tool leaves the workpiece for various t_0/t_w.

3.5. Discussion

Machining induced stress can influence the workpiece across the thickness and may reach the interface of the workpiece and the substrate in the thin workpiece. The high t_0/t_w and high E_W/E_S conditions have greatest effect on the machined workpiece especially in the combination when the $t_0/t_w = 1$ and the compliant substrate with the stress profile generally having wider range of stress values from the machined surface down to the bottom. Hence, these conditions, due to the large variation of the stress across the thickness, may produce larger deflection of the workpiece shape. In the case of lower thickness ratio, the less variation of the stress mainly due to the dissipation of the stress to other parts of the thicker workpiece condition. These effects are observed in both the stress at steady state cutting condition and the residual stress after the tool leaves the workpiece. Moreover, it can be seen from the simulation results that the stress is tensile in the machined surface under steady state cutting condition but turned to be compressive after the tool leaves the workpiece regardless the ratio of t_0/t_w and E_W/E_S. In the thicker workpiece, the depth of the loading from the tool is highly affected only down to about 3-5 μm below the machined surface. This is also seen in the residual stress where the high stress value only occurs down to the same depth which is insignificant to the thickness. The stiffer substrate ($E_S > E_w$) produces less variation of the stress values across the thickness due to the stress dissipation by the stiff substrate. In general, the effect of the different elastic modulus is more obvious when the thickness ratios are 0.5 and 1. The results show a significant effect of the workpiece thickness and the influence of the substrate properties on the stress profile in the micro-cutting process.

4. Summary

The main conclusions of this paper are:

a. The cutting force and thrust force values extracted from the simulation are relatively comparable for the thick and thin workpiece and for different variation of elastic modulus, although as the t_0/t_w becoming larger the forces range is broader for different elastic modulus ratio due to the higher displacement experienced by the substrate.
b. The stress profile is broader when $t_0/t_w = 0.5$ and 1 in steady state cutting conditions and after the tool leaves the workpiece implying that as the machined workpiece become thinner, the stress is more significant not only on the machined surface but also it reaches the bottom of the workpiece.
c. The stiffer substrate produces less variation of the stress across the workpiece thickness while more compliant substrate produces broader stress variation.

References

[1] Sakai, M., 2010, "Substrate-affected contact deformation and hardness of an elastoplastic film coated on purely elastic substrates," Surface and Coatings Technology, **204**(8), pp. 1247–1251.
[2] Saptaji, K., and Subbiah, S., 2013, "Orthogonal Microcutting of Thin Workpieces," Journal of Manufacturing Science and Engineering, **135**(3), p. 031004.
[3] Kazban, R. V, Vernaza Pena, K. M., and Mason, J. J., 2008, "Measurements of forces and temperature fields in high-speed machining of 6061-T6 aluminum alloy," Experimental Mechanics, **48**(3), pp. 307–317.
[4] De Meter, E. C., 2005, "Characterization of the quasi-static deformation of LAAG joints adhering machined steel surfaces," Journal of Manufacturing Science and Engineering, **127**(2), pp. 350–357.
[5] Ramesh, K., Huang, H., Yin, L., and Yui, A., 2004, "Surface waviness controlled grinding of thin mold inserts using chilled air as coolant," Materials and Manufacturing Processes, **19**(2), pp. 341–354.

[6] Lesuer, D. R., Kay, G. J., and LeBlanc, M. M., 2001, "Modeling large strain, high rate deformation in metals," Modelling the Performance of Engineering Structural Materials II. Proceedings of a Symposium, TMS - Miner. Metals & Mater. Soc, Warrendale, PA, USA, pp. 75–86.
[7] Gupta, N. K., Iqbal, M. A., and Sekhon, G. S., 2006, "Experimental and numerical studies on the behavior of thin aluminum plates subjected to impact by blunt- and hemispherical-nosed projectiles," International Journal of Impact Engineering, **32**(12), pp. 1921–1944.
[8] "http://www.matweb.com."
[9] Johnson, G. R., and Cook, W. H., 1985, "Fracture characteristics of three metals subjected to various strains, strain rates, temperatures and pressures," Engineering Fracture Mechanics, **21**(1), pp. 31–48.
[10] Zorev, N. N., 1963, "Interrelationship between shear processes occuring along tool face and on shear plane in metal cutting," In Proceedings of the International Research in Production Engineering Conference, ASME, New York, pp. 42–49.
[11] Bourne, K. A., Kapoor, S. G., and DeVor, R. E., 2011, "Study of the mechanics of the micro-groove cutting process," Proceedings of the ASME 2011 International Manufacturing Science and Engineering Conference, MSEC2011.
[12] Shih, A. J., 1996, "Finite element analysis of orthogonal metal cutting mechanics," International Journal of Machine Tools and Manufacture, **36**(2), pp. 255–273.
[13] ABAQUS, 2009, Abaqus 6.9 documentation.
[14] Ruud, C. O., 1986, "Residual stress measurements," ASM handbook / prepared under the direction of the ASM International Handbook Committee, Materials Park, OH : ASM International, 1986-.
[15] Jawahir, I. S., Brinksmeier, E., M'Saoubi, R., Aspinwall, D. K., Outeiro, J. C., Meyer, D., Umbrello, D., and Jayal, A. D., 2011, "Surface integrity in material removal processes: Recent advances," CIRP Annals - Manufacturing Technology, **60**(2), pp. 603–626.
[16] Jacobus, K., DeVor, R. E., and Kapoor, S. G., 2000, "Machining-induced residual stress: experimentation & modelling," Journal of Manufacturing Science and Engineering, Transactions of the ASME, **122**, pp. 20–31.